HHS Public Access

Author manuscript

Drug Alcohol Depend. Author manuscript; available in PMC 2015 July 01.

Published in final edited form as:

Drug Alcohol Depend. 2015 July 1; 152: 102–108. doi:10.1016/j.drugalcdep.2015.04.015.

A Hyper-connected but Less Efficient Small-world Network in the Substance-Dependent Brain

Ze Wang[1,2,3,*], **Jesse Suh**[3,4], **Zhengjun Li**[3], **Yin Li**[1], **Teresa Franklin**[3], **Charles O'Brien**[3], and **Anna Rose Childress**[3]

[1] Zhejiang Key Laboratory for Research in Assessment of Cognitive Impairments, Philadelphia, PA 19104, USA

[2]Center for Cognition and Brain Disorders, Hangzhou Normal University, Philadelphia, PA 19104, USA

[3] Department of Psychiatry, Perelman School of Medicine, University of Pennsylvania, Philadelphia, PA 19104, USA

[4] VISN-4 Mental Illness Research, Education and Clinical Center, VA Medical Center, Philadelphia, PA 19104, USA

Abstract

Background—The functional interconnections of the addicted brain may differ from the non-addicted population in important ways, but prior analytic approaches were usually limited to the study of connections between a few number of selected brain regions. Recent approaches enable examination of the vast functional interactions within the entire brain, the functional connectome (FCM). The purpose of this study was to characterize FCM alterations in addiction using resting state functional Magnetic Resonance Imaging (rsfMRI) and to assess their relations to addiction-related symptoms.

Methods—rsfMRI data were acquired from 20 chronic polydrug users whose primary diagnosis was cocaine dependence (DRUG) and 19 age-matched non-drug using healthy controls (CTL). FCM was assessed using graph theoretical analysis.

Results—Among the assessed 90 brain subdivisions, DRUG showed stronger functional connectivity. After controlling functional connectivity difference and the resultant network density, DRUG showed reduced communication efficiency and reduced small-worldness.

Conclusions—The increased connection strength in drug users' brain suggests an elevated dynamic resting state that may enable a rapid, semi-automatic, execution of behaviors directed toward drug-related goals. The reduced FCM communication efficiency and reduced small-

[*]Correspondence should be addressed to Ze Wang, Ph.D, 126 Wenzhou Rd, Building 7, MRI Room, Affiliated Hospital, Hangzhou Normal University, Hangzhou, Zhejiang, China 310015, zewang@mail.med.upenn.edu, or redhatw@gmail.com.

Contributors: ZW designed and conducted the study; ZW, YL, ZL analyzed data, ZW, TF, ARC interpreted data; ZW, JS, TF, COB, ARC prepared, reviewed, and approved the manuscript. Dr. Wang and Dr. Childress had full access to all the data in the study and took responsibility for the integrity of the data and the accuracy of the data analysis.

Conflict of Interest: No conflict declared.

worldness suggest a loss of normal inter-regional communications and topology features that makes it difficult to inhibit the drug seeking behavior.

Keywords

drug addiction; cocaine; resting state fMRI; functional connectome

1. Introduction

Drug addiction is a chronic relapsing disorder that affects the brain structures and functions (Koob and Volkow, 2010). While functional neuroimaging investigations have contributed significant information about addiction-related brain differences in focal brain regions and systems (Hong et al., 2009; Janes et al., 2012; Lindsey et al., 2003; Ma et al., 2010; Volkow et al., 2003), less work has been done examining the complex brain network and connectivity patterns of multiple brain regions, though those properties may reflect the (acute or chronic) impact (Bullmore and Sporns, 2009; Rubinov and Sporns, 2010) of drug exposure. Assessing them may provide new insights about the addicted brain state, offering an expanded framework for examining the neuronal underpinnings of substance dependence.

Brain networks can be assessed using fMRI (Bullmore and Sporns, 2009; Rubinov and Sporns, 2010) and graph theoretical analysis (GTA) (Watts and Strogatz, 1998). Reliable functional connectome (FCM) topological properties have been demonstrated in the healthy brain(Achard et al., 2006) with high test-retest stability(Braun et al., 2012; Wang et al., 2011). In drug addiction, FCM analysis has been applied in heroin and methamphetamine abusing populations, and these published reports showed inconsistent results with both larger or smaller FCM properties in drug addicted brain (Ahmadlou et al., 2013; Jiang et al., 2013; Liu et al., 2011a). Meanwhile, several seed-based FC studies have shown poor connectivity between frontal and limbic areas (Gu et al., 2010; Hong et al., 2009; Kelly et al., 2011; Ma et al., 2010). It is then not clear whether FCM analysis will echo with the prior seed-based connectivity analysis results, or whether new patterns will be evident when the brain's interconnections are considered as a whole. In the current study, we examined addiction-related FCM using resting-state fMRI (rsfMRI) in a drug abusing sample of patients with a primary diagnosis of cocaine dependence (DRUG) and compared to FCM in a demographically-similar control group (CTL) to identify potential addiction-related variations.

2. Materials and methods

2.1. Subjects

Twenty DRUG patients (age 42.15±4.3 (mean ± standard deviation (std)), years of education 10.07±1.7 all African-American men) with a DSM-IV diagnosis of cocaine dependence and 19 and age/ethnicity/race-matched controls (CTL) were recruited from the local community of West Philadelphia (age, 39.9±4.5; education, 14.9±2.9 yrs; all African-American men). The two groups were matched in age (p=0.13 for the age difference). CTL had more years of education than DRUG (p=0.0006). Detailed demographic data were listed in Table 1. The patients were treatment-seeking for cocaine-addiction, but defined by the

M.I.N.I. (Sheehan et al., 1998), 6 patients had a diagnosis of alcohol dependence; 2 with alcohol abuse; 1 had marijuana dependence; and 2 had marijuana abuse. Therefore, for inferences in this initial connectome study, they are best-characterized as poly-substance abusers.

All subjects underwent full physical and psychological examinations. Severity of drug dependence was assessed using the Addiction Severity Index (ASI) (McLellan et al., 1980). Patients were not using medications that may cause sedation or are known to modify brain dopamine systems during the previous 60 days; had no cardiovascular, hematologic, hepatic, renal, neurological or endocrinological abnormalities; no history of head trauma or injury; no gambling problems; no history of psychosis or organic brain syndrome unrelated to drug abuse; and no other severe psychiatric disorders, with the exception of dependence on other substance as described above. Patients had 4-8 days of residential stabilization prior to study entry, during which they were drug-free, verified by urine drug screens. CTL were not dependent on any substances including alcohol and nicotine. Drug craving scores were recorded before the MRI scan using the Brief Substance Craving Scale (Somoza et al., 1995).

2.2. MRI data acquisition

MR imaging was conducted in a 3-T whole-body scanner (Siemens, Erlangen, Germany). High-resolution structural images were acquired for spatial brain normalization using a 3D MPRAGE sequence (TR/TE/TI = 1620/3/950ms). rsfMRI images were acquired using a gradient-echo echo-planar-imaging sequence with parameters of: TR/TE = 2s/30ms, FOV = 220×220 mm^2, matrix = 64×64×32, slice thickness= 4.5 mm. Participants were asked to lie still in the scanner at rest and keep their eyes open. 180 images were acquired.

2.3. Image preprocessing

All data preprocessing was performed using SPM8 (http://www.fil.ion.ucl.ac.uk/spm)-based batch scripts (Wang et al., 2008) with the following steps: motion correction, coregistration, and normalization. Next, rsfMRI images were detrended to remove the linear and quadratic signal drift. Head motion time courses, the mean cerebral spinal fluid (CSF) and mean white matter signal were regressed out from each voxel's time series (Fair et al., 2008). The volume-to-volume displacement of each rsfMRI acquisition was calculated using the method proposed in (Power et al., 2012). The mean displacement of all acquisitions was taken as an indicator of the gross motion. A two-sample t-test was performed and showed no significant motion difference between patients and controls (p=0.25). To further reduce motion effects, acquisitions with a volume-to-volume displacement >0.5 were excluded from further FCM analysis (Power et al., 2012). The number of excluded images didn't show significant difference between the two groups (p=0.4). rsfMRI images were also filtered using a passband of 0.01Hz-0.08Hz. No spatial smoothing was applied to prevent introducing artificial correlations. The rsfMRI images were then registered into the high-resolution structural images and subsequently into the MNI standard space using SPM8 (Ashburner, 2007).

2.4. Anatomical parcellation

rsfMRI time series were extracted from the preprocessed images from 90 regions (45 for each hemisphere, see Table 2 for the subdivision labels) as defined by the automated-anatomically-labeled (AAL) brain template (Tzourio-Mazoyer et al., 2002), which is widely used in FCM analysis (Achard et al., 2006). Since some of our resting state fMRI acquisition didn't cover the entire cerebellum, we didn't consider the cerebellum subdivisions in AAL during FCM analysis. The gravity center of each subdivision was used as its surrogate node.

2.5. Network construction

Pearson correlation coefficients (CC) of rsfMRI timecourses were calculated for any pair of nodes. CC matrix was converted into a binary one using a threshold from 0.05 to 0.60 with a step of 0.01. The resulting binary matrix was used to build an undirected graph model G of the brain network (Watts and Strogatz, 1998). To visualize the FCM difference, a $p < 0.01$ (corrected for multiple comparisons using the false discovery rate (FDR) theory (Genovese et al., 2002)) was used to find the corresponding CC threshold for all subjects and the maximum of them (across all subjects) (which was 0.26) was used as the final threshold to dichotomize the 90×90 CC matrix and build the FCM.

FCM topological properties rely on the network density, which is reliant on the connectivity strength. Populational connectivity difference may then affect topological FCM comparisons. To control network density difference, the CC matrix was also thresholded to have the same network density (sparsity) and was used for the subsequent FCM analysis. While sparsity thresholding would affect FCM properties especially when it is high, a between-group comparison should still be valid if the same threshold is used for both groups.

2.6. FCM measures

The following FCM measures (Rubinov and Sporns, 2010) were calculated using the brain connectivity toolbox (www.brain-connectivity-toolbox.net/):

2.6.1. Cost—The number of connections to a node was counted as its degree. The mean degree of all nodes reflects the density of a network.

2.6.2. Segregation measures—Segregation refers to splitting the brain into functionally specialized but densely interconnected sub-regions (a sub-group of nodes here). Each such sub-group is referred to as a clique. The clustering coefficient of a node is the fraction of its neighbors that are also neighbors of each other (Watts and Strogatz, 1998); the mean clustering coefficient C_p of all nodes reflects the prevalence of local clusters ("cliquishness") of the network: $0 \leq C_p \leq 1$, with $C_p=1$ meaning each node is connected to all others. Local efficiency of a node is the average inverse shortest-path length (Latora and Marchiori, 2001) between the node pairs in the node's nearest neighborhood. Mean local efficiency (mLE) of all nodes is related to C_p.

2.6.3. Measures of network integration—Integration means unifying different sub-regions (a sub-group of nodes here) into a single functional entity and is usually

characterized with paths that connect distinct nodes (Rubinov and Sporns, 2010) with shorter path representing stronger integration potential. The characteristic path length L_p is defined as the average shortest-path length between all pairs of nodes in the network (Watts and Strogatz, 1998). A related integration measures is the global efficiency (GE) E_{global} and is defined as the average inverse shortest-path length (Latora and Marchiori, 2001).

2.6.4. *Small-worldness* is computed by comparing the real network to random networks with the same number of nodes and average degree

$$\sigma = \frac{C_p^{real}}{C_p^{rand}} / \left(\frac{L_p^{real}}{L_p^{rand}} \right)$$

(Humphries and Gurney, 2008; Watts and Strogatz, 1998). Random networks were generated using the random rewiring procedure proposed in (Maslov and Sneppen, 2002). Small-worldness measures the segregation and integration balance. A "small-world network" has $\sigma > 1$, which is more clustered (with higher C_p) than random networks, but has approximately the same L_p as that of a random network (Watts and Strogatz, 1998).

2.7. Patient versus (vs) control comparisons

DRUG-CTL FCM difference was examined using two sample-t testing at each threshold. Age was included as nuisance covariates.

2.8. FCM vs drug dependence and craving

To explore the potential clinical significance of FCM in the polydrug-dependent brain, regression analyses were performed to assess the associations between the mean degree, local efficiency, global efficiency, and small-worldness and severity of cocaine dependence, alcohol dependence, marijuana dependence (or abuse), and smoking (cigarette per day and smoking durations). Cocaine dependence level was from 0 to 9; alcohol/marijuana dependence (abuse) were included as binary scores indicating either dependence or non-dependence.

2.9. Network visualization

A mean CC matrix was calculated for patients and controls separately, and was dichotomized using the maximum of all subjects' FDR 0.05-corrected thresholds of each group. The resultant group level FCMs were displayed using BrainNet Viewer (http://www.nitrc.org/projects/bnv/)(Xia et al., 2013).

3. Results

3.1. Group level FCM appearance and differences

All abbreviations for brain regions are defined in Table 2. Bilaterality was assumed if unilaterality was not specified in the following text.

Figure (Fig.) 1 shows the nonthresholded mean CC matrix of CTL (Fig. 1A) and DRUG (Fig. 1B), their histograms (Fig. 1C and 1D, respectively), and their anatomical projection

when the connectivity matrix was thresholded using a FDR 0.05 corrected CC threshold. Both the CC matrices (Fig. 1A, 1B) and the histograms (Fig. 1C, 1D) demonstrate that DRUG had on average stronger inter-regional correlations than CTL. DRUG patients showed higher node degrees (bigger node size) and more connections (as reflected by lines) than controls (Fig. 1E, 1F). Patients showed fewer node clusters than controls (4 vs 6) as indicated by different node colors in Fig. 1E and 1F. Fig. 1G (and Table 2) shows the nodes with significant patient-control degree difference ($p<0.05$ with Bonferroni correction). A homogeneous node increase between 18-21 was observed in supplementary motor area (SMA), post-central gyrus (PoCG), and in the inferior cortex from insula to Rolandic operculum (ROL), temporal cortex, to fusiform, lingual cortex, calcarine cortex (CAL), then to cuneus, and to visual cortex.

3.2. FCM differences at different thresholds

Fig. 2 shows FCM measures derived from individual-level FCM built with different thresholds. Fig. 2A shows that the mean degree decreased with the CC threshold and patients showed significantly ($p<0.001$) higher degree than controls for all tested thresholds. According to (Watts and Strogatz, 1998), there exists an up-limit, R_{max} for the threshold above which small-worldness is not estimable. The mean network degree decreases to log (N) (N=90 in this study) when the threshold reaches R_{max}. In this study, when the threshold was >0.55, the mean degree of controls was < log (N)=4.50, indicating $R_{max}\approx 0.55$ for controls. R_{max} for patients was larger than 0.55 since patients had larger node degrees than controls at any CC threshold. So the results were presented using a threshold range of 0.05 to 0.55. After controlling the functional connectivity strength difference by using the sparsity threshold, DRUG showed lower local communication efficiency (Fig. 2B) when sparsity was <15%, and lower global communication efficiency (Fig. 2C) when sparsity was >31%. For most of assessed sparsity thresholds, DRUG showed reduced small-worldness (Fig. 2D).

3.3. Relations of FCM properties to drug use measures

After correcting for multiple comparisons, no significant associations between the FCM properties and drug addiction clinical measures were observed.

4. Discussion

Here we report that a cohort of DRUG patients (cocaine-dependence treatment-seekers with several comorbid substance use disorders), had a hyperconnected resting brain network with higher wiring cost, but lower communication efficiency and reduced small-worldness compared to an age and gender matched CTL group. The hyperconnected resting FCM in DRUG may suggest an elevated dynamic resting state in the addicted brain. Small-worldness is related to communication efficiency. The reduced small-worldness and communication efficiency suggest a loss of normal inter-regional communications that may underlie the loss of cognitive control and inhibition in drug addiction.

Nodes with increased degree located in the visual sensorimotor network, including insula, ROL (Rolandic operculum), temporal cortex, fusiform, visual area, and cuneus, as well as

SMA (supplementary motor area). Temporal cortex and FFG (fusiform gyrus) lie within the memory/learning circuit, and INS(insula) are substrates of motivation and drive, which are altered in drug addiction(Koob and Volkow, 2010; Naqvi et al., 2007; Volkow et al., 2003). Other nodes including PoCG(postcentral gyrus), SMA, ROL, CAL(calcarine cortex), CUN(cuneus), LING(lingual gyrus), MOG(middle occipital gyrus), and SOG(superior occipital gyrus) are regions within the motor, visual, and spatial perception/imagination areas, and the increased connections therein might reflect a result of the altered memory/learning function and motivation/drive function, which both involve functions in the three areas. Hyperactivity in the reward system is observed in drug addiction (Volkow et al., 2003), but we did not observe node-degree changes in DRUG patients in basal ganglia, thalamus, and amygdala. Future studies using fMRI data acquired during a drug cue paradigm might reveal differences in the FC of these regions. Moreover, we did not see node-degree increase in ACC, SFC, and MSFC, which are regions within the control circuit. A cardinal feature of addiction is the inability to inhibit behavior (Jovanovski et al., 2005). Although our findings using rsfMRI differ from the confirmed addiction-related activations using task fMRI in those regions (Childress et al., 2008; Childress et al., 1999; Volkow et al., 2006), they may simply indicate an equally-communicated inhibition circuit in the patients' and controls' brain during rest. Nevertheless, higher degrees were found in patients at nodes distributed in all other places. These findings suggest that a loss of inhibition in the addicted brain might be a result of the grossly increased FC outside the medial prefrontal area. Increased FC within the medial prefrontal regions might restore balance and enhance the inhibition control in drug addicted brain.

Our FCM topology findings are partly consistent with previous FCM studies. Higher FCM node degrees in abstinent heroin-dependent patients was reported by Yuan et al in a small study with 11 patients and 11 controls (Yuan et al., 2010). The reduced small-worldness was consistent with the findings in heroin-dependent individuals in (Jiang et al., 2013). While Gu et al. showed reduced inter-regional FC in cocaine users using the seed-based FC analysis (Gu et al., 2010), the seed-based FC cannot characterize the FCM topology. Our FCM analysis results suggest that the loss of inhibition or cognitive control in cocaine patients may be related to a loss of FCM topology properties rather than an alteration of the connection strength. Another explanation for the paradox of having both increased connection strength but reduced network metrics could be that the connection strength is elevated to compensate the loss of FCM communication efficiency.

We didn't find significant relations between FCM measures and clinical measures for addiction, which is probably due to the small sample size included in the current study. A future study would be assessing the clinical meanings of FCM using larger sample sizes. The intensely inter-connected brain of addicted individuals might help to explain the clinical phenomenology of the disorder (ritualized, efficient pursuit of drug). One interesting future study would be to assess whether effective medications like methylphenidate, which has been shown to alter resting FC in cocaine addiction(Konova et al., 2013), could impact the hyperconnections in drug users. Moreover, as resting activity has been shown to be predictive of task activations (Liu et al., 2011b; Zou et al., 2013), another future investigation would be using resting FC or FCM properties to predict task or drug-cue

induced brain activations or alternatively using it to reduce inter-subject variations in functional neuroimaging addiction studies.

One limitation of current study is that there was a significant difference of education years between the two groups, which should be considered in future assessment. Nevertheless, we showed similar findings in a preliminary version of this study presented in a conference when more subjects were included to match the education level though age was not matched therein (Wang, 2014). Another limitation is that as with any cross-sectional imaging study addicted adults, it is not possible to know whether the observed brain patterns are a result of drug exposure, or whether they preceded or even pre-disposed the addiction -- or whether they represent some interaction of these factors. In the future, longitudinal studies (repeated scans) of FCM in addicted individuals would also be helpful in determining whether the observed patterns of connectivity are a stable feature in addiction, or whether they show change with time since last drug-use, or with extended periods of recovery. Much larger studies, well beyond the scope of this initial observation, would enable statistical comparisons of the various subgroups (e.g., cocaine, alcohol, marijuana, and nicotine) represented within the current DRUG cohort, vs. CTL. The current study thus does not allow attributions of the findings to one particular drug class, though our between-group effects remained when covarying out some drug use factor such as smoking measures (data not shown).

In summary, DRUG patients showed a hyperconnected and less efficient FCM. The study offers a foundation for explicit attempts to link other addiction features (e.g., reward sensitivity, difficulty with inhibiting) to FCM. FCM studies may be a useful tool for characterizing the addicted state, and a screen for potential anti-addiction therapeutics.

Acknowledgement

This work was supported by NIH grants: 1R56DA036556, 5R01DA025906, 5R33DA026114, 1R03DA029677, and 5P50DA012756, the CURE Addiction Center of Excellence: Brain Mechanisms of Relapse and Recovery grant from the Commonwealth of Pennsylvania and by the Hangzhou Qianjiang Endowed Professor Program and the Youth 1000 Talent Program of China. The authors thank Dr. Anita Hole and Dr. Kathleen Marquez at the Department of Psychiatry, University of Pennsylvania for assistance.

Role of Funding Source: Nothing declared

Reference

Achard S, Salvador R, Whitcher B, Suckling J, Bullmore E. A resilient, low-frequency, small-world human brain functional network with highly connected association cortical hubs. The Journal of neuroscience. 2006; 26:63–72. [PubMed: 16399673]

Ahmadlou M, Ahmadi K, Rezazade M, Azad-Marzabadi E. Global organization of functional brain connectivity in methamphetamine abusers. Clinical neurophysiology. 2013; 124:1122–1131. [PubMed: 23332777]

Ashburner J. A fast diffeomorphic image registration algorithm. Neuroimage. 2007; 38:95–113. [PubMed: 17761438]

Braun U, Plichta MM, Esslinger C, Sauer C, Haddad L, Grimm O, Mier D, Mohnke S, Heinz A, Erk S, Walter H, Seiferth N, Kirsch P, Meyer-Lindenberg A. Test-retest reliability of resting-state connectivity network characteristics using fMRI and graph theoretical measures. NeuroImage. 2012; 59:1404–1412. [PubMed: 21888983]

Bullmore E, Sporns O. Complex brain networks: graph theoretical analysis of structural and functional systems. Nat Rev Neurosci. 2009; 10:186–198. [PubMed: 19190637]

Childress AR, Ehrman RN, Wang Z, Li Y, Sciortino N, Hakun J, Jens W, Suh J, Listerud J, Marquez K, Franklin T, Langleben D, Detre J, O'Brien CP. Prelude to passion: limbic activation by "unseen" drug and sexual cues. PLoS One. 2008; 3:e1506. [PubMed: 18231593]

Childress AR, Mozley PD, McElgin W, Fitzgerald J, Reivich M, O'Brien CP. Limbic activation during cue-induced cocaine craving. The American journal of psychiatry. 1999; 156:11–18. [PubMed: 9892292]

Fair DA, Cohen AL, Dosenbach NUF, Church JA, Miezin FM, Barch DM, Raichle ME, Petersen SE, Schlaggar BL. The maturing architecture of the brain's default network. Proceedings of the National Academy of Sciences of the United States of America. 2008; 105:4028–4032. [PubMed: 18322013]

Genovese CR, Lazar N, Nichols TE. Thresholding of Statistical Maps in Functional Neuroimaging Using the False Discovery Rate. NeuroImage. 2002:870–878. [PubMed: 11906227]

Gu H, Salmeron BJ, Ross TJ, Geng X, Zhan W, Stein EA, Yang Y. Mesocorticolimbic circuits are impaired in chronic cocaine users as demonstrated by resting-state functional connectivity. Neuroimage. 2010; 53:593–601. [PubMed: 20603217]

Hong LE, Gu H, Yang Y, Ross TJ, Salmeron BJ, Buchholz B, Thaker GK, Stein EA. Association of nicotine addiction and nicotine's actions with separate cingulate cortex functional circuits. Arch Gen Psychiat. 2009; 66:431–441. [PubMed: 19349313]

Humphries MD, Gurney K. Network 'small-world-ness': a quantitative method for determining canonical network equivalence. PLoS One. 2008; 3:e0002051. [PubMed: 18446219]

Janes AC, Nickerson LD, Frederick Bde B, Kaufman MJ. Prefrontal and limbic resting state brain network functional connectivity differs between nicotine-dependent smokers and non-smoking controls. Drug Alcohol Depen. 2012; 125:252–259.

Jiang G, Wen X, Qiu Y, Zhang R, Wang J, Li M, Ma X, Tian J, Huang R. Disrupted topological organization in whole-brain functional networks of heroin-dependent individuals: a resting-state FMRI study. PLoS One. 2013; 8:e82715. [PubMed: 24358220]

Jovanovski D, Erb S, Zakzanis KK. Neurocognitive deficits in cocaine users: a quantitative review of the evidence. Journal of clinical and experimental neuropsychology. 2005; 27:189–204. [PubMed: 15903150]

Kelly C, Zuo XN, Gotimer K, Cox CL, Lynch L, Brock D, Imperati D, Garavan H, Rotrosen J, Castellanos FX, Milham MP. Reduced interhemispheric resting state functional connectivity in cocaine addiction. Biol Psychiatry. 2011; 69:684–692. [PubMed: 21251646]

Konova AB, Moeller SJ, Tomasi D, Volkow ND, Goldstein RZ. Effects of methylphenidate on resting-state functional connectivity of the mesocorticolimbic dopamine pathways in cocaine addiction. JAMA psychiatry. 2013; 70:857–868. [PubMed: 23803700]

Koob GF, Volkow ND. Neurocircuitry of addiction. Neuropsychopharmacology. 2010; 35:217–238. [PubMed: 19710631]

Latora V, Marchiori M. Efficient behavior of small-world networks. Phys Rev Lett. 2001; 87:198701. [PubMed: 11690461]

Lindsey KP, Gatley SJ, Volkow ND. Neuroimaging in drug abuse. Curr Psychiat Rep. 2003; 5:355–361.

Liu JX, Qin W, Yuan K, Li J, Wang W, Li Q, Wang YR, Sun JB, von Deneen KM, Liu YJ, Tian J. Interaction between Dysfunctional Connectivity at Rest and Heroin Cues-Induced Brain Responses in Male Abstinent Heroin-Dependent Individuals. Plos One. 2011a; 6:e23098. [PubMed: 22028765]

Liu X, Zhu XH, Chen W. Baseline BOLD correlation predicts individuals' stimulus-evoked BOLD responses. Neuroimage. 2011b; 54:2278–2286. [PubMed: 20934521]

Ma N, Liu Y, Li N, Wang CX, Zhang H, Jiang XF, Xu HS, Fu XM, Hu X, Zhang DR. Addiction related alteration in resting-state brain connectivity. Neuroimage. 2010; 49:738–744. [PubMed: 19703568]

Maslov S, Sneppen K. Specificity and stability in topology of protein networks. Science. 2002; 296:910–913. [PubMed: 11988575]

McLellan AT, Luborsky L, Woody GE, O'Brien CP. An improved diagnostic evaluation instrument for substance abuse patients. The Addiction Severity Index. The Journal of Nervous and Mental Disease. 1980; 168:26–33. [PubMed: 7351540]

Naqvi NH, Rudrauf D, Damasio H, Bechara A. Damage to the insula disrupts addiction to cigarette smoking. Science. 2007; 315:531–534. [PubMed: 17255515]

Power JD, Barnes KA, Snyder AZ, Schlaggar BL, Petersen SE. Spurious but systematic correlations in functional connectivity MRI networks arise from subject motion. Neuroimage. 2012; 59:2142–2154. [PubMed: 22019881]

Rubinov M, Sporns O. Complex network measures of brain connectivity: uses and interpretations. NeuroImage. 2010; 52:1059–1069. [PubMed: 19819337]

Sheehan DV, Lecrubier Y, Sheehan KH, Amorim P, Janavs J, Weiller E, Hergueta T, Baker R, Dunbar GC. The Mini-International Neuropsychiatric Interview (M.I.N.I.): the development and validation of a structured diagnostic psychiatric interview for DSM-IV and ICD-10. Journal of Clinical Psychiatry. 1998; 59(Suppl 20):22–33. quiz 34-57. [PubMed: 9881538]

Somoza, E.; Dyrenforth, S.; Goldsmith, J.; Mezinskis, J.; Cohen, M. In search of a universal drug craving scale; Annual Meeting of the American Psychiatric Association; Miami, FL. 1995.

Tzourio-Mazoyer N, Landeau B, Papathanassiou D, Crivello F, Etard O, Delcroix N, Mazoyer B, Joliot M. Automated anatomical labeling of activations in SPM using a macroscopic anatomical parcellation of the MNI MRI single-subject brain. Neuroimage. 2002; 15:273–289. [PubMed: 11771995]

Volkow ND, Fowler JS, Wang GJ. The addicted human brain: insights from imaging studies. Journal of Clinical Investigation. 2003; 111:1444–1451. [PubMed: 12750391]

Volkow ND, Wang GJ, Telang F, Fowler JS, Logan J, Childress AR, Jayne M, Ma Y, Wong C. Cocaine cues and dopamine in dorsal striatum: mechanism of craving in cocaine addiction. The Journal of neuroscience. 2006; 26:6583–6588. [PubMed: 16775146]

Wang JH, Zuo XN, Gohel S, Milham MP, Biswal BB, He Y. Graph theoretical analysis of functional brain networks: test-retest evaluation on short- and long-term resting-state functional MRI data. PLoS One. 2011; 6:e21976. [PubMed: 21818285]

Wang Z, Aguirre GK, Rao H, Wang J, Fernández-Seara MA, Childress AR, Detre JA. Empirical optimization of ASL data analysis using an ASL data processing toolbox: ASLtbx. Magnetic Resonance Imaging. 2008; 26:261–269. [PubMed: 17826940]

Wang, Z.; Suh, JJ.; Young, KA.; Monge, Z.; O'Brien, CP.; Childress, AR. A Hyper-connected and More Resilient Small-world Network in the Cocaine-Dependent Brain; 2014 College on Problem of Drug Dependence Annual Meeting; Puerto Rico. 2014.

Watts DJ, Strogatz SH. Collective dynamics of 'small-world' networks. Nature. 1998; 393:440–442. [PubMed: 9623998]

Xia M, Wang J, He Y. BrainNet Viewer: a network visualization tool for human brain connectomics. PLoS One. 2013; 8:e68910. [PubMed: 23861951]

Yuan K, Qin W, Liu J, Guo Q, Dong M, Sun J, Zhang Y, Liu P, Wang W, Wang Y, Li Q, Yang W, von Deneen KM, Gold MS, Liu Y, Tian J. Altered small-world brain functional networks and duration of heroin use in male abstinent heroin-dependent individuals. Neurosci Lett. 2010; 477:37–42. [PubMed: 20417253]

Zou Q, Ross TJ, Gu H, Geng X, Zuo XN, Hong LE, Gao JH, Stein EA, Zang YF, Yang Y. Intrinsic resting-state activity predicts working memory brain activation and behavioral performance. Hum Brain Mapp. 2013; 34:3204–3215. [PubMed: 22711376]

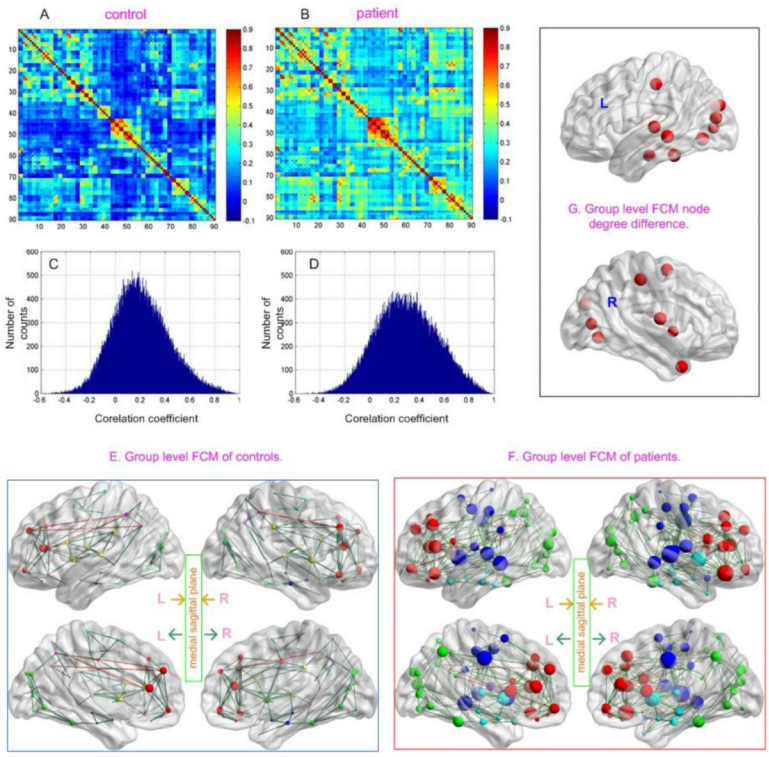

Fig 1.

Resting FCM of DRUG patients and the age-matched controls (CTL). A) and B) The average inter-regional correlation coefficient (CC) matrix of CTL, and DRUG, respectively; C) and D) The histogram of the CC matrices shown in A and B, respectively; E) and F) The average FCM of CTL and DRUG, respectively; G) Network nodes with significantly higher degree in DRUG patients than in CTL (defined by $p<0.05$, bonferroni corrected for 90 comparisons). Network nodes are projected into the brain surface based on their spatial locations. As indicated by the inset in the middle of E and F, the top two sagittal slices of E and F are the pictures projected to the left (L) and right (R) brain hemisphere, respectively; the left and right sagittal slices on the bottom row are the projections of the left and right hemisphere to the middle sagittal plane, respectively. Node color in E and F indicates different modules (cliques). Red lines and dark green lines represent long (>=75 mm) and short (<75 mm) distance connections, respectively. Node size was in proportional to the node degree or node degree difference (in G).

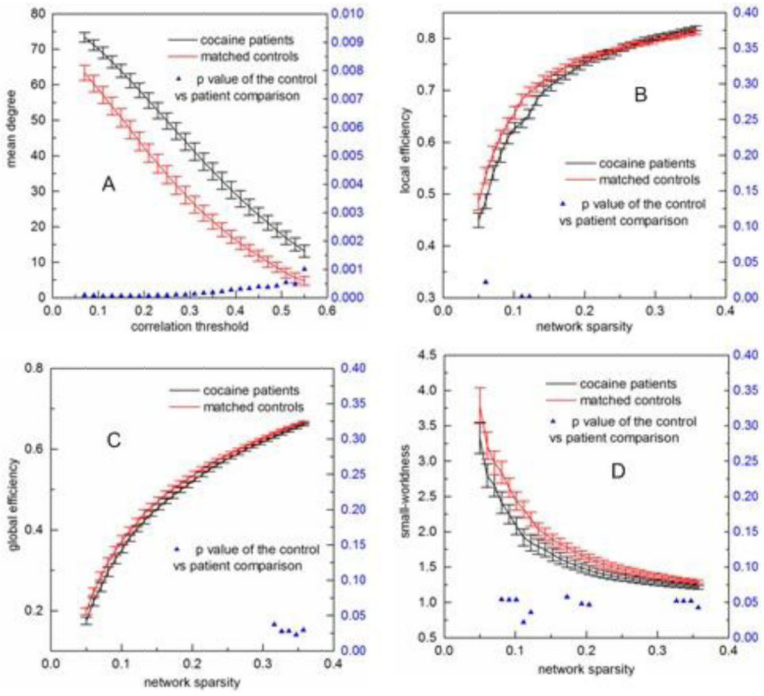

Fig 2.

FCM measures calculated at different correlation coefficient thresholds for DRUG patients (the black line) and controls (the red line) and their statistical comparison results (two sample t-testing). A) Mean network degree, B) local efficiency, C) global efficiency, D) small-worldness. Error bars indicate standard error within each group at each threshold value. The blue triangles display the two-sample t-testing p values.

Table 1

Demographic data for participants.

	Patients (n=20)	**Controls (n=19)**
Age (yrs)	42.15±4.3	39.9±4.5
Education (yrs)	12.07±1.7	14.9±2.9
Gender	20 males	19 males
Cocaine dependence severity	7.26±1.76	0
Alcohol dependence severity	2.68±2.54	0
Marijuana dependence or abuse	2	0
Drug craving score	0~3, 0.28±0.83	0
Cigarette per day	7.67±6.0	0
Smoking duration (yrs)	15.61±12.1	0

Table 2

AAL brain subdivision names, abbreviations and the node degree difference between cocaine patients and controls (patient-control).

Abbr	Full name	Δdeg	Abbr	Full name	Δdeg
PreCG	Precentral gyrus		LING	Lingual gyrus	21.8(L),19.8(R)
SFC	Superior frontal cortex		SOG	Superior occipital gyrus	20.1(L)
SOFC	Superior orbito-frontal cortex		MOG	Middle occipital gyrus	20.3(L)
MFC	Middle frontal cortex		IOG	Inferior occipital gyrus	
MiOFC	Middle orbito-frontal cortex		FFG	Fusiform gyrus	21.4(L)
IFCoper	Inferior frontal cortex (opercular)		PoCG	Postcentral gyrus	20.4(L),20.6(R)
IFCtria	Inferior frontal cortex (triangular)		SPC	Superior parietal cortex	
LOFC	Lateral orbito-frontal cortex		IPC	Inferior parietal cortex	
ROL	Rolandic operculum	21.0(R)	SMG	SupraMarginal gyrus	
SMA	Supplementary motor area	20.1(R)	ANG	Angular gyrus	
OLF	Olfactory		PCUN	Precuneus	
MSFC	Medial superior frontal cortex		PCL	Paracentral Lobule	
MOFC	Medial orbito-frontal cortex		CAU	Caudate	
REC	Rectus		PUTA	Putamen	
INS	Insula	18.4(R)	PALL	Pallidum	
ACC	Anterior cingulate cortex		THA	Thalamus	
MCC	Middle cingulate cortex		HES	Heschl's gyrus	
PCC	Posterior cingulate cortex		STC	Superior temporal cortex	20.4(L)
HIPP	Hippocampus		STOP	Superior temporal pole	
PHIPP	ParaHippocampus	20.0(L)	MTC	Middle temporal cortex	21.5(L)
AMY	Amygdala		MTPO	Middle temporal pole	20.5(R)
CAL	Calcarine cortex	18.9(L),19.2(R)	ITC	Inferior temporal cortex	
CUN	Cuneus	18.6(L),20.8(R)			

Δdeg mean the patient minus control degree difference.